Fission-stability of high-K states in superheavy nuclei

J. Khuyagbaatar[a]

GSI Helmholtzzentrum für Schwerionenforschung, 64291 Darmstadt, Germany

Abstract Fission is the one of the primary radioactive decay modes for the heaviest nuclei and ultimately determines the existence of the heaviest elements on a macroscopic time scale, e.g., $\geq 10^{-14}$ s. The present experimental data on the decay properties of the heaviest nuclei with proton numbers 102–118 and/or of neutron numbers up to 177 show that fission occurs occasionally. This confirms that shell structure plays an essential role for their stability against fission. The shell effect on fission manifests in both collective and single-particle ways, which can experimentally be studied in decays of even–even, odd-A and odd–odd nuclei. At the same time, high-K states formed in couplings of quasiparticles are also known to be stable against fission. However, detailed knowledge and theoretical descriptions on a retardation effect/strength of high-K quantum number on fission are still scarce. In the present work, fission from high-K states are discussed and described within the semi-empirical approach. Fission half-lives are calculated for various high-K states, which have been theoretically predicted to exist in Fm-Rf ($Z = 100$–104) and Hs-Ds ($Z = 108$–112). The results are found to be in line with the available experimental findings, and also leading to different intriguing predictions, e.g., high-K states in superheavy nuclei tend to be more stable against fission compared to their ground states.

1 Introduction

Fission, in which a heavy nucleus splits into smaller fragments is a complex process having dynamical and statistical natures, where a large number of internal degrees of freedom are involved [1–3]. The most stable configuration of a nucleus against fission is its ground state, where no excitation energy is available. Fission probability increases greatly as a function of excitation energy, which usually spreads over intrinsic excitation modes (e.g., rotational, vibration and single particle levels). Fission was experimentally observed and studied in 1930's [4,5] from the decay of such an excited nucleus, and only properly interpreted in 1939 [6,7]. One year later, the spontaneous fission (SF) from the ground state of primordial nucleus was discovered [8]. Since then, the essential impact of fission on the stability of heavy nuclei has been understood [9].

In the classical representation of the atomic nucleus as a structureless charged nuclear liquid drop [7,9], which consists of Z protons and N neutrons, heavy nuclei with, e.g., $Z > 100$ would be unstable against fission on a timescale of $\leq 10^{-14}$ s, which is often expressed as a lower limit (i.e., isotopic border) for the existence of an atom [10]. However, it turned out that nucleons occupy quantified discrete orbitals inside the nucleus. This shell structure of nucleons has a great impact on fission in both collective and single-particle ways.

A collective effect appears on the potential energy surface of a nucleus by the changing shape and height of the potential-energy barrier [11,12], which results in an increased stability against fission. Understanding of this property led to the prediction of the superheavy nuclei (SHN) [13] with $Z > 103$ [14], which can exist on a timescale much longer than 10^{-14} s [15–18].

Presently, the heaviest nuclei with proton or neutron numbers up to $Z = 118$ or $N = 177$ are known. Their half-lives are found to be in the range of 10^{-6}–10^5 s [19,20]. This indicates that a limit for the existence of superheavy atomic species is not yet reached. At the same time, the possible existence of SHN with very long half-lives that may lead to naturally occurring superheavy elements is still under question. However, the presently available experimental fission data show that the single-particle nature of the shell structure can greatly enhance the fission stability in addition to the 'collective' effect [21].

The effect of a single proton and/or neutron occupying the outermost orbitals in odd-A and odd–odd nuclei can be

^{a} e-mail: J.Khuyagbaatar@gsi.de (corresponding author)

seen in their experimental SF half-lives, which are significantly longer than those in the neighboring even–even nuclei in which all its nucleons are paired and thus have a total spin of zero [22]. Indeed, theoretical descriptions for such a single-particle effect on the fission exist [23–25]. However, the predictive powers of theoretical descriptions on SF half-lives of odd-A and odd–odd nuclei still need to be improved.

Furthermore, single-particle effects on fission can appear in the cases of even–even nuclei when there is excitation energy and deformation. This can occur when nucleons from a broken pair are again coupled but from different single-particle orbitals [26]. A configuration formed in such a coupling, which is referred as a multi-quasiparticle (qp) state may result in a large total angular momentum (hereafter: a total spin) and projection onto the symmetry axis. The latter value, which is usually expressed as a K quantum number according to the Nilsson notations [27], is the sum of each total spin projection of the involved single-particle orbitals. Such high-K states are located at certain excitation energies which should favor direct fission, however, are nevertheless known to be stable against fission and exist as isomeric states in many heavy nuclei [26,28–31]. One should note that such multi-qp states with high-K can be populated and experimentally studied in even–even, odd-A and odd–odd heavy nuclei, which can be synthesized via fusion-evaporation reactions [19,20,31–34].

Fission stability of a high K-state is the one of longstanding and demanding topics in both experimental and theoretical research in the region of heavy nuclei [30,35–39]. Earlier theoretical works anticipated that high-K states can be extremely stable against fission by having partial half-lives much longer than their ground states [35]. However, it was predicted to occur only in the region of heavy nuclei around $Z = 100$ and $N = 152$, e.g., in ^{250}Fm and ^{254}No, where K-isomeric states were known at that time. However, the experimental observations of direct fission from K-isomeric states in ^{256}Fm [40] and ^{254}No [41] with partial half-lives shorter than those for the ground states did not confirm the above theoretical prediction. On the other hand, these findings were diverging only slightly from the theory, because such a weak effect of the high-K number on the fission stability was also anticipated to occur but in heavier nuclei [36]. Accordingly, theory and experiment did not provide the promise to observe a high-K isomeric state in SHN, which could live longer than its ground state.

The situation has since been changed with the experimental observation of a long-lived α-decaying K-isomeric state in ^{270}Ds [42]. A theoretical problem of the fission stability of high-K states has been reconsidered [28]. Furthermore, experimental observations of long-lived K-isomeric states decaying by electromagnetic transitions in ^{250}No [43–46] and ^{254}Rf [47], and by α-particle emission in ^{266}Hs [48], reveal the great impact of a high-K number on fission. Exact

qp configurations of these states are scarcely known, and are occasionally assigned with theoretical inputs [28,49–51]. Nevertheless, from these cases, one can conclude that the nucleus can be very stable against fission at a relatively high excited state, if the K number is high. However, direct fission of these states is yet to be observed experimentally, which sets a limit on the estimation of the fission-stability gain compared to their ground states.

Overall, despite great experimental and theoretical efforts on the study of K-isomeric states in heavy nuclei [25,35–39], understanding of the effect of a high-K number on fission and on the stability of an excited state remains incomplete. As a consequence of this circumstance is then a lack of theoretically calculated fission half-lives for many high-K qp-states, which were theoretically predicted to exist in SHN.

The present work aims at calculating the fission half-lives for various theoretically predicted high-K states in even–even SHN. To reach this goal, the problem of fission from high-K states is discussed and described within a recently suggested semi-empirical approach, which is based on a semi-classical theory of fission by Hill and Wheeler. The novelty this semi-empirical approach brings is an account of fission-barrier shape, which has been previously successful in descriptions of the electron-capture delayed fission process [52] and the spontaneous fission of the ground-state [53] in heavy nuclei.

2 Stability of high-K states against electromagnetic transitions

The stability, i.e., half-life of a multi-qp state having a high spin, a high K quantum number, and located at a certain excitation energy is well studied in the region of medium-mass and deformed nuclei [26,30]. Fission probabilities of such nuclei are negligibly low not only at their ground states but also at their excited states with energies up to several MeV below which most of the high-K states occur. Hence, their instabilities are determined mainly by electromagnetic decays; γ-ray emission and internal conversion. These are the common de-excitation modes for all intrinsic excited states, which have either low K, or $K = 0$. The electromagnetic transitions with different multipolarities that occur between such states remove the excitation energy and angular momentum (if available) [54]. In the de-excitation of a high-K state, the γ-transition should also remove/lower an initial high-K quantum number. This has an effect on the decay rate of a γ-transition, which becomes retarded compared to one with $\Delta K = 0$.

Commonly, a retardation effect that takes a place in any radioactive decay (e.g., electromagnetic and α decay) is studied by extracting the so-called hindrance factor. The hindrance factor is defined as a ratio of the experimental (hin-

dered) and calculated (unhindered) half-lives of a radioactive decay. The calculated value can be taken from either an empirical expression or pure theoretical calculation, but in both cases a retardation effect is not accounted for yet.

In the case of electromagnetic decays of high-K states, theoretical half-lives for γ-transitions without a retardation effect caused by $\Delta K > 0$ from Weisskopf is used. Accordingly, the effect of a high-K quantum number on the decay rate of the electromagnetic transition is expressed via the hindrance factor defined as a ratio of half-lives from the experiment and the Weisskopf estimate. Indeed, the experimental half-lives of high-K states are longer than the ones given by Weisskopf, which reveals their isomeric nature [31].

The electromagnetic decay of a high-K state can proceed by different de-excitation paths in which an initial K value will be reduced by different amounts, ΔK. This occurs because in the deformed nucleus large number of low-lying excited states with either $K = 0$ or low-K are available. Each γ-transition removing a particular ΔK is characterized by its own partial half-life and the hindrance factor. Decades ago, a well pronounced relation between the ΔK and its corresponding hindrance factor (F_K) had been recognized [55,56]. This relation expressed as $\log(F_K) \sim \Delta K$ is commonly used for a description of the experimental data from which the semi-empirical expression for the estimate of F_K is extracted. Such a semi-empirical fit is still used for the interpretation of the experimental data.

3 Definition of fission-hindrance for an excited state with a high-K configuration

In the case of high-K states in the heaviest nuclei, in addition to the electromagnetic transitions, one should also consider other types of radioactive decay modes such as α-particle emission and fission [28]. Compared to the electromagnetic decay, fission will not remove/release a partial ΔK value. Thus, an initial high-K value can be considered to be conserved until the collective motion of nucleons that initiate fission will alter it. In other words, a nucleus' shape evolution along the axial symmetry axis is frozen for a while because of a high-K quantum number. Hence, the effect of a high-K qp-configuration on fission can straightforwardly be expressed by its absolute value, i.e., $\Delta K = K$.

A retardation effect of fission caused by high-K value often discussed by comparing the fission half-lives of a high-K state and the ground state [30,37]. To some extent, this has a theoretical basis, where both values can be calculated [35–37]. Experimentally, only two cases in which such a "hindrance factor" can be extracted are known. Thus, the hindrance factor "defined" in this way is ineffective for discussions for the majority of experimental data on the K-isomeric states. Therefore, it is preferable to introduce a differently

defined fission hindrance that can firmly quantify the effect of high-K and can be useful for discussing the experimental data.

Let us express the fission hindrance, $F_H(K)$, in a similar way as any other hindrance factors that are used in the radioactive decays, i.e.,

$$F_H(K) = \frac{T_f^{exp}(J, K)}{T_f^{cal.}(J, 0)} \tag{1}$$

where $T_f^{exp}(J, K)$ is the experimentally measured fission half-life of an excited state (E^*) formed from the coupling of a multi-qps with a total spin of J and a quantum number of K. Furthermore, for simplicity, we will use these variables without their units ($\hbar$, reduced Planck constant). $T_f^{cal.}(J, 0)$ is the theoretical half-life calculated for a state with spin J and an excitation energy of E^*. This is the same state as high-K, but with $K = 0$. In this regard, such a hypothetical state can be interpreted as being an intrinsic high-J state with $K = 0$, which are common and of frequent occurrence in deformed nuclei. Now, one needs to calculate the fission half-life for such an excited state.

4 Theoretical description of the fission process and its probability

Modern theoretical approaches describe fission as nuclear shape evolution on the multi-dimensional potential energy surface for which calculations involve a large number of the internal degrees of freedom. In such a treatment, the fission half-life is extracted by calculating an action integral for a particular path on potential energy surface that leads to fission [57]. However, despite such an expansive knowledge and description of fission dynamics [3], the predictive powers of theoretical calculations for various fission-related observables (e.g., half-life) remain to be improved. More importantly, theoretical approaches do not provide any calculated result, which can be taken as aforementioned unhindered fission half-lives.

An alternative solution can be found in the classical theoretical approach, where the fission probability is calculated as a transmission over/through an inverted harmonic oscillator, i.e., a parabolic-shaped barrier introduced by Hill and Wheeler [9]. Let us briefly provide a reminder on the main concept of this classical approach.

In the first theoretical model, where fission was described as a collective motion of nucleons in which the shape of the nucleus evolves from a sphere to an elongated shape, a potential energy barrier for the fission process was introduced [7]. Since then the fission barrier is commonly expressed as its height and shape, and these became the main quantities for the description of the fission process in a particular
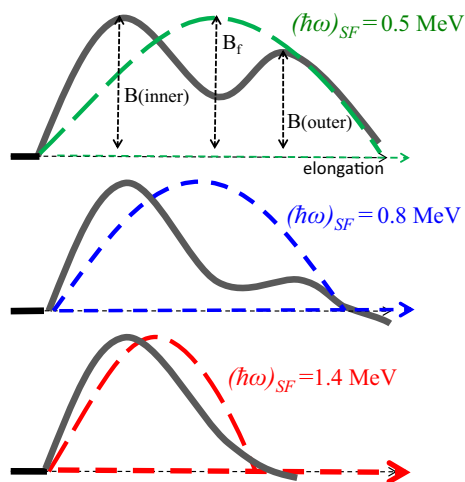
Fig. 1 Schematic illustrations of evolution of the fission-barrier shapes from double-hump to single-hump. Dashed curves demonstrate approximate parabolic barriers with heights of B_f and widths of $(\hbar\omega)_{SF}$ for a description of the spontaneous fission. See text for details
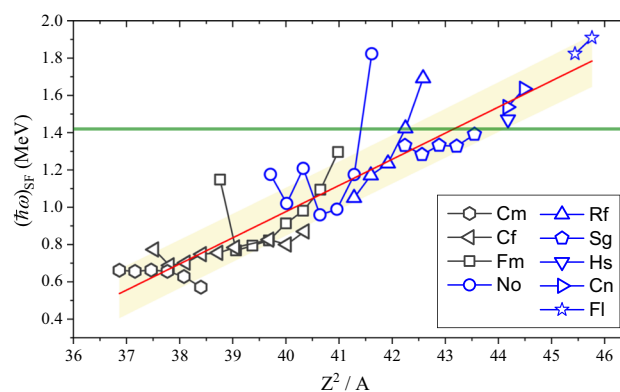

Fig. 2 Extracted SF barrier widths [53] for the approximate parabolic barriers with the calculated heights from the FRLDM [59] as function of the fissility parameters of nuclei, Z^2/A. A fit to these data is shown within a 68% prediction level. A horizontal line indicates a $(\hbar\omega)_{SF}$ value at 1.42 MeV above which no outer barrier would exist. See text for details

nucleus. With such a barrier, the theoretical calculations of fission-related quantities (e.g., SF half-life, T_{SF}) of the atomic nucleus became possible within the framework of liquid drop model (LDM), where the fission-barrier shape was described by a parabola [9].

The fission probability according to Hill–Wheeler is expressed as

$$T \approx \{1 + exp[2\pi(B_f - E^*)/\hbar\omega]\}^{-1}, \qquad (2)$$

where $\hbar\omega$ is the curvature energy which quantifies the width of the parabolic barrier (see Fig. 1) and B_f its height.

The relation between the fission half-life, T_f, and transmission coefficient can be taken as;

$$T_f^{cal.} = \ln(2)/(nT), \qquad (3)$$

where n is the frequency of barrier assaults ($\omega/2\pi$) for the nucleus undergoing fission, which is associated with $\hbar\omega$. A value for n can be derived from the width of the thermal neutron resonances as described in Ref. [58], and taken as 10^{14} s^{-1}.

Despite the great success of the LDM, it has failed to explain some experimental observations on the fission process. Those deviations have been elucidated by introducing nuclear shell effects into the LDM [11].

As a result of this merger, the shell structure has been found to greatly impact the shape evolution of the nucleus (see Ref. [17] and references in there). For instance, the fission barrier along the elongation axis does not have a single-hump as the LDM predicts, but rather, more complex shapes, e.g., double-hump (see Fig. 1) [11,12,17,18,59].

Hence, the calculation of fission probability, i.e., T_f over the multi-humped barriers became a challenging problem in quantum mechanics for which various solutions have been

suggested [12] (see references in there). However, the main issue for obtaining a reasonably good prediction for the experimental T_{SF} is not primarily a matter of how the penetrability is being calculated, but rather how well the height and shape of the fission barrier are calculated.

It is worth noting that the fission-barrier heights in the heaviest nuclei are often extracted from the experimental fission related observable by using a particular theoretical description. Therefore, an adequate comparison of the "experimental" fission-barrier heights with theoretically calculated ones is often impossible [3].

Nevertheless, the initially suggested one dimensional fission barrier with a certain height and shape is still valid for description of the fission process in nuclei within wide ranges of Z and N. Moreover, the results from modern theoretical calculations in which fission is described by all possible pathways on the potential energy surface towards the scission points are often represented by a one dimensional fission barrier (e.g., fission-barrier height).

Presently, fission-barrier heights calculated within various theoretical approaches are available. This circumstance enables a broad application of the Hill-Wheeler expression for descriptions of various quantum penetration processes in nuclear physics, such as the fusion of two colliding nuclei [60] and the nucleosynthesis r-process [61].

Recently, this classical approach has been successfully used for descriptions of the probability of the electron-capture delayed fission [52], and SF half-lives [53]. A novelty brought for this approach was the semi-empirically estimated fission-barrier shape. Let us now attempt to calculate the unhindered fission half-lives within this new approach. For this, one has to consider the results obtained in those previous works, which will be discussed the following sections.

4.1 The spontaneous fission half-lives and barriers

Experimental data on the fission of heavy nuclei show strong variations of fission-barrier height and shape as functions of both Z and N. The double-humped fission barrier, which is strongly pronounced in nuclei with $Z \approx 90-94$ is theoretically predicted to become a single-humped in nuclei with $Z = 104$ [17,62,63].

In Fig. 1, such a transition of the fission-barrier shape is shown schematically. Spontaneous fission from such differently shaped barriers can be approximated and described by a parabola, which represents a single hump, as shown in Fig. 1. In all cases, the heights of parabolic barriers, B_f, correspond to the height of the inner barrier. Since the nuclear motion for SF passes over all possible structures on the shape of the fission barrier, which characterizes a total/main fission path on the potential energy surface [18,57,59,64], the lowering of the outer-barrier height relative to the inner-barrier can be represented by a parabolic barrier with a narrower width. Accordingly, by describing the experimentally measured SF half-lives of the heaviest nuclei with Eqs. (2) and (3), and with theoretically predicted B_f values, the curvature energies, i.e., barrier widths can be extracted as done in Ref. [53].

The extracted curvature energies for SF, $(\hbar\omega)_{SF}$, of approximate parabolic barriers with B_f from the most commonly used finite-range liquid-drop model (FRLDM) [59] are shown in Fig. 2 as a function of the fissility parameter, Z^2/A [7,22,58,65]. A well pronounced linear trend is fit using the following equation

$$(\hbar\omega)_{SF} = 0.14025 \times Z^2/A - 4.6335. \tag{4}$$

This finding, i.e., a linear trend can be explained within the parabolic-shape approximation sketched in Fig. 1. The lowest values in Fig. 2 corresponding to Cm ($Z = 96$) isotopes indicate broader parabolic barrier shapes, which approximately describe the experimentally known multi-humped barriers. On the other hand, larger $(\hbar\omega)_{SF}$ values in heavier nuclei implies that the barrier shape becomes narrower, which can be explained as a decrease of the outer-barrier effect (see Fig. 1).

The majority of theories predict a single humped fission barrier for ^{256}Rf [17,62,63], thus its $(\hbar\omega)_{SF} = 1.42$ MeV value shown in Fig. 2 can be regarded as a benchmark for nuclei without an outer-fission barrier. Most of the SHN shown in Fig. 2 have $(\hbar\omega)_{SF} \geq 1.42$ MeV, which suggests that their barrier shapes are likely to be single-humped. Hence, the parabolic shaped barrier appear to be a well-justified approximate for a description of fission in SHN within the present semi-empirical approach with fission-barrier heights from FRLDM.

On the other hand, $(\hbar\omega)_{SF}$ values in Fm-Rf isotopes, in which most experimental data on K-isomeric states are known, are less than 1.42 MeV. Thus, in these nuclei the
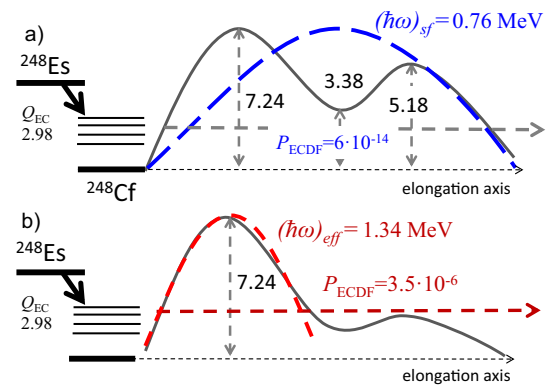

Fig. 3 Schematic illustrations of the ECDF process in ^{248}Es. Theoretical $Q_{EC}(^{248}$Es) and fission barrier heights (in MeV) for ^{248}Cf were taken from [66] and [64], respectively. The double-hump structure of the fission barrier is highlighted by the solid lines. Parabolic barriers with $B_f = 7.24$ MeV and with differently extracted widths are shown by dashed curved lines. The widths deduced from the SF half-life of ^{248}Cf and of the ECDF probability of ^{248}Es are denoted as $(\hbar\omega)_{SF}$ (**a**) and $(\hbar\omega)_{eff}$ (**b**), respectively. The calculated P_{ECDF} values corresponding to these two different barriers are given. Dashed arrows mark a passage 'over' the parabolic barriers. See text for details

effect of the outer barrier could still be significant, but primarily for fission from the ground state. Regarding high-K states, which lies at excitation energies about/above 1 MeV, however, the situation may be a different.

A common impact of excitation-energy and outer-barrier effects on fission has been recently investigated in the description of the electron-capture delayed fission (ECDF) process within the approximate parabolic barrier approach as introduced above and applied in this work.

4.2 Fission from excited states: electron-capture delayed fission

An example of ECDF in ^{248}Es is shown schematically in Fig. 3. After the EC decay of ^{248}Es ($Q_{EC} = 2.98$ MeV according to finite-range droplet model [66]), excited states (up to 2.98 MeV) in ^{248}Cf are populated, and a portion of them may undergo a direct fission instead of populating the ground state via electromagnetic transitions. Most of these excited intrinsic states have either $K \approx 0$ or low K. The theoretical fission-barrier structure for the ground state of ^{248}Cf according to the FRLDM [59] is also shown in Fig. 3a. The penetration over such a double-humped fission barrier is approximated by a parabolic barrier with a height taken from the FRLDM.

A curvature energy of $(\hbar\omega)_{SF} = 0.76$ MeV was extracted from the experimental SF half-life of ^{248}Cf [67] according to the above discussion (see also Fig. 2). With a curvature energy of 0.76 MeV, the ECDF probability is calculated to be only 6×10^{-14} [52], which is negligibly small compared to the experimental value of 3.5×10^{-6} [68].

A solution for this ambiguity was found by suggesting that the outer barrier does not have a large effect on fissions from excited states. This means that the effective parabolic fission barrier, which is relevant for ECDF is narrower than the one for SF. With such an assumption, an effective curvature energy of $(\hbar\omega)_f = 1.34$ MeV was then extracted from the experimental ECDF probability of 3.5×10^{-6} [68], and was attributed to correspond mostly to the inner-barrier width (see Fig. 3b). With such a parabolic barrier, all known ECDF probabilities were successfully described in Ref. [52], and the impact of the fission-barrier shape on fission from excited states has been revealed. Moreover, a further narrowing of such an effective barrier, i.e., $(\hbar\omega)_f > 1.34$ MeV was noticed to take place in heavier nuclei, e.g., at least in Fm isotopes. This is the same conclusion, which was derived from the above-analysis of SF half-lives of all known even–even nuclei (see Fig. 2 and Ref. [53]).

In cases of K-isomeric states, typical excitation energies (e.g., 2-qp states have ≈ 1 MeV) are smaller than in cases of ECDF (e.g., < 3 MeV in ^{248}Cf). Therefore, in Cf isotopes, the outer barrier may still have an effect on the fission probability of high-K states, which may require the use of $(\hbar\omega)_f < 1.34$ MeV. However, by considering the above-mentioned further narrowing of an effective barrier in Fm isotopes [52], and of SF barriers in heavier nuclei, one can conclude that $(\hbar\omega)_f = 1.34$ MeV can still be used efficiently for a description of fission from excited states of even–even nuclei, of elements heavier than Cf/Fm; but only in cases where the corresponding $(\hbar\omega)_{SF}$ is less than 1.34 MeV.

Finally, we have established all of the necessary ingredients for the calculation of unhindered fission half-lives of high-K states in nuclei with $Z \geq 100$ based on Eqs. (2)–(4).

1. Fission-barrier heights are taken from FRLDM [59].
2. Curvature energy of a parabolic fission barrier is taken as:
   - $(\hbar\omega)_f = 1.34$ MeV for $(\hbar\omega)_{SF} < 1.34$ MeV
   - $(\hbar\omega)_f = (\hbar\omega)_{SF}$ for $(\hbar\omega)_{SF} > 1.34$ MeV (see Eq. 4)
3. Excitation energies and qp-configurations of high-K states can be taken from experimental data and/or theoretical predictions.

5 Extraction of the experimental fission-hindrance factors

Now after being able to calculate the unhindered fission half-life, we can extract the fission hindrances in the cases of K-isomeric states, where their direct fission is known. Such cases are known only in ^{256}Fm and ^{254}No, where well-assigned $K^\pi = 7^-$ and 8^- states have $T_f^{exp}(7) =$
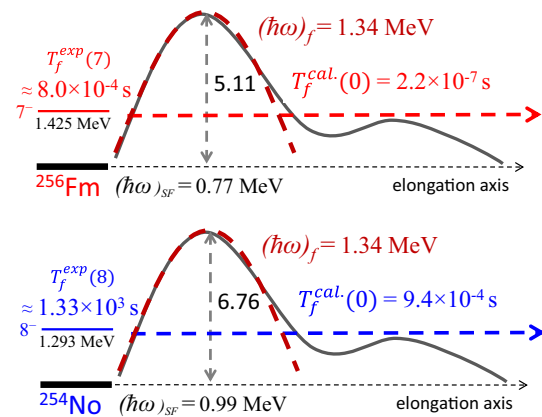

Fig. 4 Schematic illustrations of fission from K-isomeric states in ^{256}Fm and ^{254}No. Experimental K^π, excitation energies and fission half-lives of these states are taken from Refs. [40,41]. Parabolic barriers with theoretically calculated heights from Ref. [59] and $(\hbar\omega)_f = 1.34$ MeV, which are used for calculation of unhindered fission half-lives of from excited states are illustrated by dashed curves. Unhindered fission half-lives from high-K states are given. Dashed arrows mark a passage 'over' the parabolic barriers. See text for details

$8^{+88}_{-7} \times 10^{-4}$ s, [40] and $T_f^{exp}(8) = (1.33 \pm 0.8) \times 10^3$ s, [41], respectively.

In Fig. 4, schematic drawings for fission of these two K-isomeric states over effective parabolic fission barriers are shown. The experimental and theoretical data on the K-isomeric states and fission barriers are also given. In both ^{256}Fm and ^{254}No, the ground-state SF half-lives are measured. This results in extracted $(\hbar\omega)_{SF}$ values of 0.77 MeV and 0.99 MeV, respectively, which are less than 1.34 MeV. As stated above, their effective parabolic fission-barrier widths for a description of unhindered fission half-lives can be taken as $(\hbar\omega)_f = 1.34$ MeV.

Then, by using Eqs. (2), (3) and the barrier heights from FRLDM [59], unhindered fission half-lives of 2.2×10^{-7} s and 9.4×10^{-4} s were calculated for the 7^- and 8^- states, respectively. These values and the experimental fission half-lives of these K-isomeric states result in $F_H(7) = 3.6 \times 10^3$ and $F_H(8) = 1.4 \times 10^6$ for ^{256}Fm and ^{254}No, respectively.

Thus, we extract fission-hindrance factors in a similar manner as for electromagnetic decay. This enables an examination of strength of the K-hindrance on fission via a search for a relation between $\log(F_H(K))$ and K.

5.1 Fission-hindrance factor dependence on K number

Extracted two hindrance factors are plotted in Fig. 5 as a function of ΔK. As we have agreed, fission hindrance of a high-K state formed in qp couplings can be quantified by a single ΔK value, which is equal to an initial K. These values show a linear dependence between $\log(F_H)$ and K despite their large uncertainties. The K value in ^{254}No leads to a larger F_H com-
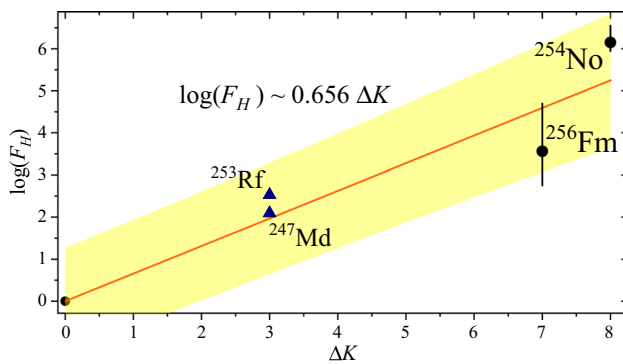
Fig. 5 Experimentally extracted fission-hindrance factors as function of ΔK. Presently estimated values for K isomeric states in ^{256}Fm and ^{254}No are shown together with hindrance factors that are suggested to originate from a $\Delta K = 3$ change in the single-particle orbitals in ^{253}Rf [69] and ^{247}Md [70]. A linear fit of the data points for ^{256}Fm and ^{254}No and the boundary point is shown within a 68% prediction level. See text for details

pared to the one for lower K state in ^{256}Fm, which seems to be reasonable. Only two data points are insufficient to draw a conclusive dependence, i.e., a linear function between $\log(F_H)$ and K values. However, one can use a boundary condition from the fission-hindrance definition. In Eq. 1, by default $F_H(0)$ is equal to 1 or $\log(F_H(0)) = 0$ because fission from intrinsic excited states have no hindrance. This normalization provides an additional "data point" that can be used in a linear-fit of two experimental points. The fit results in a function of $\log(F_H) \approx 0.656\Delta K$. Observation of such an exponential dependence between the fission-hindrance factor and K is in fact not accidental because any radioactive decay has an exponential time distribution, which defines its decay rate and stability. As an example, such relation is known in the case of electromagnetic decay of the high-K states [55,56].

The above fit, indeed, has a large uncertainty, which is mainly due to uncertainties on the experimental fission half-lives of K isomers. For a more refined definition of fit-parameters, more precise experimental data are necessary. However, experimentally, this is very difficult to achieve due to low production yields of heavy nuclei, which require long experiments with high intensity heavy-ion beams running under low fission-background conditions [37,40,41]. Nevertheless, attempts are still making [33,46]. Furthermore, in the near future, it is unlikely that new data points with lower or higher-K will be added in Fig. 5. Therefore, despite scarce experimental data, the presently suggested semi-empirical estimate can be useful for discussion and understanding of the high-K hindrance on the fission stability of SHN.

In this regard, it would be interesting to compare the presently extracted fission hindrance from the K-isomeric data with that which was recently extracted from the single-particle configuration [69]. In this work, observations of

direct fissions from two different single-particle states in ^{253}Rf were reported. A ratio of their fission half-lives was suggested to reveal differences in corresponding effects of their single-particle configurations. Such a ratio then resulted in a factor of ≈ 330, and considered as an experimental fission-hindrance value corresponding to $\Delta K = 3$. Since both states belong to the same nucleus and are close-lying, let us take the above value as being $F_H(3)$.

Another such a case was also measured in ^{247}Md [70], where the ratio of fission half-lives resulting in ≈ 120 and has been attributed to reveal the fission hindrance caused by $\Delta K = 3$. This value is slightly lower than the one measured for ^{253}Rf. Firstly, this can be due to the limited statistics of observed fission events, and secondly, may relate with a fission property of an individual nucleus ^{247}Md.

These values are plotted in Fig. 5 at $\Delta K = 3$. Remarkably, they lie very close to the linear fit. Within the present work, we will not discuss this finding in detail. However, such a similarity of fission hindrances extracted from the K-isomeric and the single-particle states can be a realistic case as the former also has single-particle nature.

On the other hand, a completely controversial interpretation for the fission hindrance that was suggested in the above-mentioned Ref. [69] for ^{253}Rf was recently given in Ref. [73]. In this work, fissions from two single-particle states in ^{253}Rf have also been measured confirming the findings in Ref. [69]. However, after the analysis of their larger statistical experimental data, which also contains new findings, the authors gave different assignments on single-particle states from which fissions originate. According to this work, a value of 0.0045 has to be attributed to a fission hindrance caused by $\Delta K = 3$ instead of the above-mentioned ≈ 330. Indeed, this does not fit into present definition of the fission hindrance. However, such an interpretation of the experimental data is extremely interesting (see also discussions on the fission-barrier shape of ^{252}Rf made in the next section) because it contradicts also to the commonly agreed (both experimentally and theoretically) point of view, where a higher J/K quantum numbers are expected to hinder the fission larger than a lower J/K [22–24]. The present findings also support this. Therefore, unambiguous experimental evidence, which would justify the statement made in Ref. [73] are highly demanded. One of the new findings in Ref. [73] was the K-isomeric state in ^{253}Rf. The existence of K-isomer state with a half-life of 0.66 ms, which is significantly longer than the ones known in ^{254}Rf [47,74], ^{255}Rf [53,75] and ^{256}Rf [76,77] is in agreement with the present estimates.

In summary, the semi-empirical approach for the estimation of the fission hindrance of a high-K state is suggested. Now, calculations of fission half-lives of known (by its electromagnetic and/or α decays), and theoretically predicted high-K states in nuclei with $Z \geq 100$ become possible.

6 Estimations of fission half-lives of theoretically predicted high-K qp-states in SHN

As mentioned in the introduction, there are many K-isomeric states in nuclei with $Z \geq 100$, which have been measured/observed mainly by their electromagnetic and α decays. Unfortunately, those experimental data often lack confidently assigned K quantum numbers and excitation energies, which are necessary for the present calculation of the fission half-life. The most reliable and comprehensive experimental data on K-isomeric states have been obtained only in cases where they can be produced with reasonably high cross-sections (larger than a few hundreds of nb), i.e., only in ^{250}Fm, ^{256}Fm, ^{252}No and ^{254}No isotopes. Many other experimental data on various K-isomeric states are only discussed and interpreted by introducing the theoretical calculations. Therefore, let us take the theoretically predicted high-K configurations and calculate fission half-lives for them.

Numerous of theoretical works devoted to predictions of various multi-qp configurations that may exist and be observed in SHN are available [28,49–51,71,78]. In general, they predict the same qp-configurations for a particular nucleus, but with different excitation energies. This results in different ordering of high-K states in a particular nucleus, which may affect the discussion on experimental data. For instance in Fig. 6, excitation energies of lower-lying 2-qp and 4-qp configurations in No and Rf isotopes from three different theoretical predictions [49,50,71] are shown. For comparisons, the experimental excitation energies of the known K-isomeric states are also shown.

As mentioned above, in most cases, an exact configuration or K value cannot be experimentally extracted, thus, such theoretical calculations are extensively involved in assignments of qp-configurations of the experimental data. Predictions on the possible qp-states in a particular nucleus primarily depend on the applied single-particle levels from a particular theory. In the case of No isotopes with $N < 152$, theories predict the same 2-qp states as being the lowest-lying K-isomeric states. Such theoretically agreed upon qp-states are often used to explain the origin of the K-isomeric states for which no experimental K-assignments are available. As an example, the known isomeric state in ^{250}No (see Fig. 6) has been suggested to have a qausi-neutron configuration of $\nu6^+(5/2^+[622] \otimes 7/2^+[624])$ for decades. Only, recently, experimental evidence for $K = 6$ has been observed for this K isomer [79]. Hence, this confirms that the theoretical predictions are valid.

In the cases of No-Rf isotopes with $N \geq 152$, the situation is different. As one can see in Fig. 6, several close- and lower-lying 2-qp configurations with different K numbers are predicted in ^{254}No ($N = 152$) and in ^{256}No ($N = 154$). This is related to the well-known shell gap at $N = 152$. Once the neutron number reaches 152, then various higher-

Fig. 6 Theoretically calculated excitation energies of various 2-qp and 4-qp states in even–even isotopes of No and Rf. These were taken from Refs. [50] (circles), [49] (squares) and [71] (triangles). Configurations: $\nu6^-(7/2^-[743] \otimes 5/2^+[622])$, $\nu6^+(5/2^+[622] \otimes 7/2^+[624])$, $\nu8_1^-(7/2^+[624] \otimes 9/2^-[734])$, $\nu8_2^-(7/2^+[613] \otimes 9/2^-[734])$, $\nu5^-(9/2^-[734] \otimes 1/2^+[620])$, $\nu4^+(1/2^+[620] \otimes 7/2^+[613])$, $\pi8^-(7/2^-[514] \otimes 9/2^+[624])$, $\pi7^-(7/2^+[633] \otimes 7/2^-[514])$, $\pi5^-(1/2^-[521] \otimes 9/2^+[624])$, $\pi\nu14^-(\pi8^- \otimes \nu6^+)$, $\pi\nu16_1^+(\pi8^- \otimes \nu8_1^-)$, $\pi\nu16_2^+(\pi8^- \otimes \nu8_2^-)$, $\pi\nu13^+(\pi5^- \otimes \nu8_2^-)$. The experimentally measured excitation energies of K-isomeric states taken from Refs. [29,72] are also shown by long horizontal-line symbols. Short horizontal-line symbols drawn at 1 MeV and 2 MeV mark the known 2-qp and 4-qp K-isomeric states, respectively, but without experimental excitation energies. The first, second and third isomeric states known in a particular nucleus are noted by m1, m2 and m3. The arrow marks a lower-limit value for energy. See text for details

lying single-particle levels close to the Fermi level are available for couplings of various quasiparticles. Accordingly, this may limit the use of theoretical predictions to interpret the experimental data. On the other hand, such theoretical predictions can be considered as there are multiple 2-qp states that may exist in a particular nucleus. Experimentally, such predictions can be confirmed, with one such example being ^{256}Rf ($N = 152$), in which two different lower-lying 2-qp K-isomeric states have been observed [76,77].

Four-qp states shown in Fig. 6 lie at excitation energies larger than 2-qp states, as such couplings require roughly about double the amount of energy for the breaking of two pairs and to allocate four unpaired nucleons in different single-particle orbitals. Occurrences of 4-qp states have been experimentally observed in ^{254}No [41], ^{254}Rf [47], ^{256}Rf [76], and recently in ^{250}No [46]. It has been found that their population probabilities in fusion-evaporation reactions, i.e., in the de-excitation of compound nucleus, are significantly
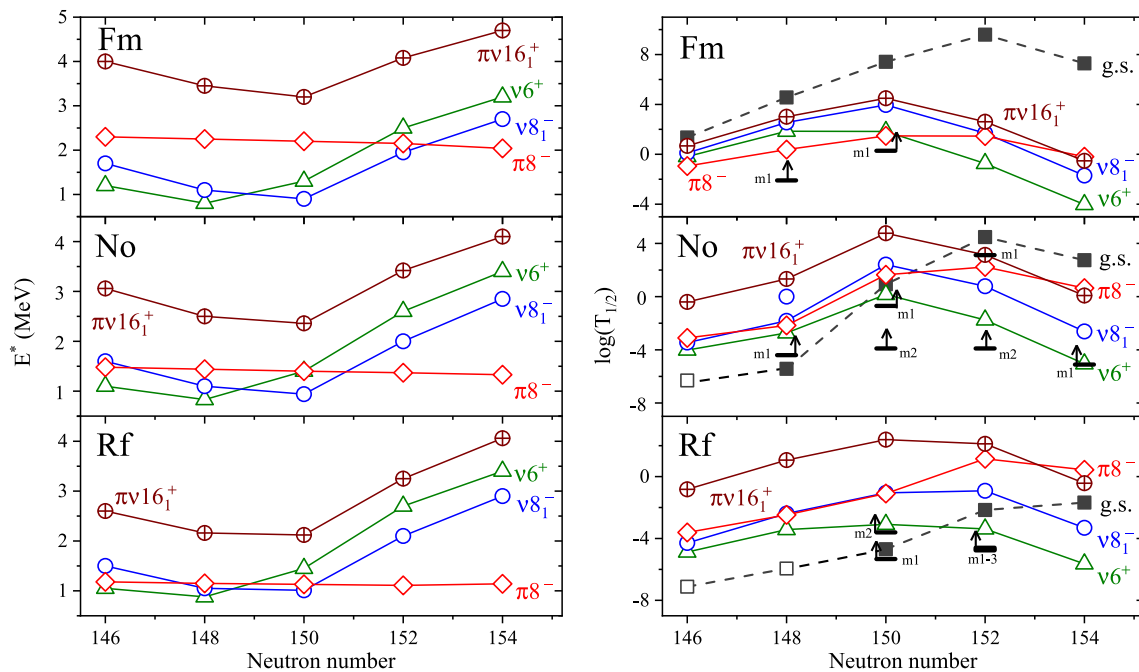
Fig. 7 Excitation energies of theoretically predicted $\nu 6^+(5/2^+[622]\otimes 7/2^+[624])$, $\nu 8_1^-(7/2^+[624] \otimes 9/2^-[734])$, $\pi 8^-(7/2^-[514] \otimes 9/2^+[624])$ and $\pi\nu 16_1^+(\pi 8^- \otimes \nu 8_1^-)$ configurations in even–even isotopes of Fm-Rf [50] (left panels). Presently calculated fission half-lives corresponding to these qp-states are shown in the right panels. The experimental partial SF half-lives [22] are shown by filled squares. SF half-lives calculated in the present work are shown by open squares.

Experimentally measured total half-lives [29,72] of K-isomeric states are shown by horizontal-line symbols. Arrows indicate that these are considered as lower limits for fission half-lives of high-K states. The isomeric states known in a particular nucleus are noted by m1, m2 and m3, where the numbers denote their occurrences as a function of the excitation energy. See text for details

lower than populations of lower-lying 2-qp states. Therefore, the experimental study of 4-qp states is more complicated, and usually their origins are assigned on the basis of their decays to lower-lying 2-qp states and/or measured excitation energies. Nevertheless, theory predicts the existence of various 4-qp states, which in general may exist but still need to be determined experimentally.

Now, let us briefly examine impact of the excitation-energy deviations between theory and experiment on the estimation of the fission half-life. As one can see in Fig. 6, the experimental and theoretical excitation energies for 2-qp and 4-qp states are in agreement within e.g., about 0.3 MeV. Such an energy deviation does not have much impact on calculated fission half-lives of high-K states. As an example, if the excitation energy of the 8^- state in ^{254}No is taken as 1.5 MeV instead of the experimental value of 1.297 MeV, then, the calculated unhindered fission half-life will be 3.6×10^{-4} s. This value is still similar (within the one order of magnitude) to the above-calculated value of 9.4×10^{-4} s with 1.297 MeV. The fission half-life of this 8^- state is mainly determined by its corresponding $F_H(8) = 10^{5.248}$ (see Fig. 5), which is much larger than the above two unhindered fission half-lives. Therefore, energy deviations between the theoretical calculations, and experimental measurements are not expected to

make a significant impact on the estimation of fission half-lives within the present approach.

In the present work, theoretical predictions from Ref. [50], where large numbers of various multi-qp states in a wide range of heavy nuclei are considered.

In the left panels of Fig. 7, excitation energies of three different 2-qp states, resulting in $K = 6$ and 8, and one 4-qp state with $K = 16$ predicted in Ref. [50] for Fm-Rf isotopes are shown. Calculated fission half-lives for these high-K states within the present semi-empirical approach are shown in right panels of Fig. 7. In order to make a comparative analysis of the fission stability, the measured SF half-lives of the ground state corresponding to each nucleus are also given. In the cases of hitherto unknown neutron-deficient ^{248}No ($N = 146$), ^{250}Rf ($N = 146$) and ^{252}Rf ($N = 148$) nuclei, SF half-lives were calculated with Eqs. (2) and (3) as described above (see also Ref. [53]). In this region of nuclei, the fission-barrier shape is suggested to be a very narrow, i.e., without the outer barrier. This was concluded on the basis of very large values of $(\hbar\omega)_{SF}$ for ^{250}No ($N = 148$), ^{254}Rf ($N = 150$) and ^{256}Rf ($N = 152$), which transcended a common trend drawn in Fig. 2. Similarly narrow fission-barrier shapes can be expected in those more neutron-deficient and hitherto unknown nuclei. Therefore, their curvature energies cannot be adequately estimated by Eq. 4. Thus, $(\hbar\omega)_{SF} =$

1.82 MeV and 1.69 MeV for ^{250}No and ^{254}Rf are adopted for those unknown No and Rf isotopes, respectively.

Let us discuss the results shown in Fig. 7 (right panels). In all Fm isotopes, fission half-lives of the 2-qp and 4-qp states are smaller than their corresponding SF half-lives. In addition, they are in agreement with experimental lower limits for the fission half-lives of K isomers. Absolute values for these limits were taken as half-lives of K isomers measured from their electromagnetic decays, thus, they are not strictly determined limits. A more "properly" extracted lower-limit value was given in ^{250}Fm [37]. This lower-limit is about $10^{6.26}$ s, which is much larger than the present results shown in Fig. 7. However, one should note that this experimental lower-limit has not been extracted on the basis of unambiguously assigned fission events to the decay of K isomer because of SF from the ground state. Thus, it might have some uncertainty. On the other hand, the fission half-lives for Fm isotopes were calculated with $(\hbar\omega)_f = 1.34$ MeV, which could overestimate the fission probability from excited states. In the case of Fm ground states, SF half-lives are strongly affected by the outer barrier. Presumably, the outer barrier still has effect on the fission probability. Meanwhile, the largest SF half-lives observed for ^{252}Fm and for ^{254}No are due to the effect of a significantly large shell gap at $N = 152$, which is theoretically predicted to result in an increased and a broadened fission-barrier height and shape, respectively.

The more pronounced effect of the $N = 152$ in the cases of No compared to Fm is seemingly due to the rapidly decreasing SF half-lives of neutron-deficient No isotopes. This can be explained by strong changes of the fission-barrier shape in the neutron-deficient No isotopes compared to the cases of Fm isotopes. For instance, the SF half-life of only 4 µs in ^{250}No ($N = 148$) can be attributed to a negligibly low outer barrier [53]. As a result of the fission-barrier shape variations of the ground and excited states, a very interesting feature in the trends of fission half-lives of high-K and ground states appears. In neutron-deficient nuclei, fission from high-K states becomes more stable compared to their corresponding ground states.

Such a behavior is in good agreement with the experimental findings for the K-isomeric state in ^{250}No. Fission from this long-lived K-isomeric state decaying via electromagnetic transitions with a half-life of ≈ 30 µs has not been observed to date. Nevertheless, this value, which is longer than its ground-state SF half-life of 4 µs, can be taken as a lower limit. Presently, the estimated fission half-life for the $K = 6$ state is longer than the ≈ 30 µs. The same is true also for other two 2-qp configurations, which may exist in ^{250}No (see Fig. 7). A direct fission from this K-isomeric state has been recently searched for, and only a lower limit of 674 µs was given [46]. This is again in line with the presently calculated value of ≈ 2 ms for the $K = 6$ configuration (see Fig. 7). Therefore, we can conclude that the presently calculated fis-

sion half-lives of high-K states are in reliable agreement with the experimental observations.

In Rf isotopes, the situation is completely opposite to Fm cases. Now, high-K states are more stable against fission compared to their ground states. At the same time, one can notice that the effect of the $N = 152$ is not as pronounced as in the case of No. Furthermore, the outer barrier is predicted to be negligible in Rf isotopes with $N < 153$, which results in shorter SF half-lives. In the cases of high-K states the fission half-lives are largely determined by great retardation effects of high-K numbers expressed by large $F_H(K)$ values. Thus, predicted fission half-lives of these high-K states are longer than the ones for SF of their ground states.

Finally, in the region of No-Rf, the ground states are predicted to become no longer the most stable configuration against fission. Instead, the high-K states are predicted to be the most stable configurations against the fission. Such an inversion of stability between the ground and high-K states is predicted to already be established in Rf isotopes. Furthermore, an inversion of stability is also valid for higher-lying 4-qp states. Moreover, 4-qp states can be more stable than the lower-lying 2-qp states, which demonstrate that the impact of high-K quantum number on the fission is greater than the effect of excitation energy and/or the ground-state fission properties. These predictions can firmly explain the experimental finding on the decay of a 4-qp state in ^{254}Rf, which lives longer than its lower-lying 2-qp state, and also its ground state [47]. Therefore, the above predictions are again in agreement with the experimental data.

In Fig. 8, the excitation energies of three different 2-qp states that result in $K = 9$ and 10 according to Ref. [50] are shown. In this region of heavy nuclei, relatively high-spin orbitals are available around their Fermi levels, and shell gaps at $N = 152$ and 162 are not as relevant. Calculated fission half-lives for these high-K states are shown in the right panels of Fig. 8 together with SF half-lives for the ground states. In most cases, the SF half-lives were calculated using Eqs. (2)–(4). All high-K states in these SHN are predicted to be more stable than their corresponding ground states. In fact, such a feature is expected since the inversion of stability had already taken place in the region of No-Rf. Supposedly, this inverted stability is a common feature of all deformed superheavy nuclei.

Superheavy nuclei are known to exist at their ground states only thanks to their shell structure. According to theory, SHN with $Z = 114, 120-126$ and $N = 184$ are predicted to be the next spherical closed shells above $Z = 82$ and $N = 126$. The closed shell has a great impact on stability of nucleus ([20] and see references therein). The SF half-lives of such a group of SHN are predicted to be much longer than the ones in the surrounding neighboring nuclei, which led in the terminology "island of stability". In this regard, a similar "philosophy" can be applied for a high-K state in deformed SHN, which is
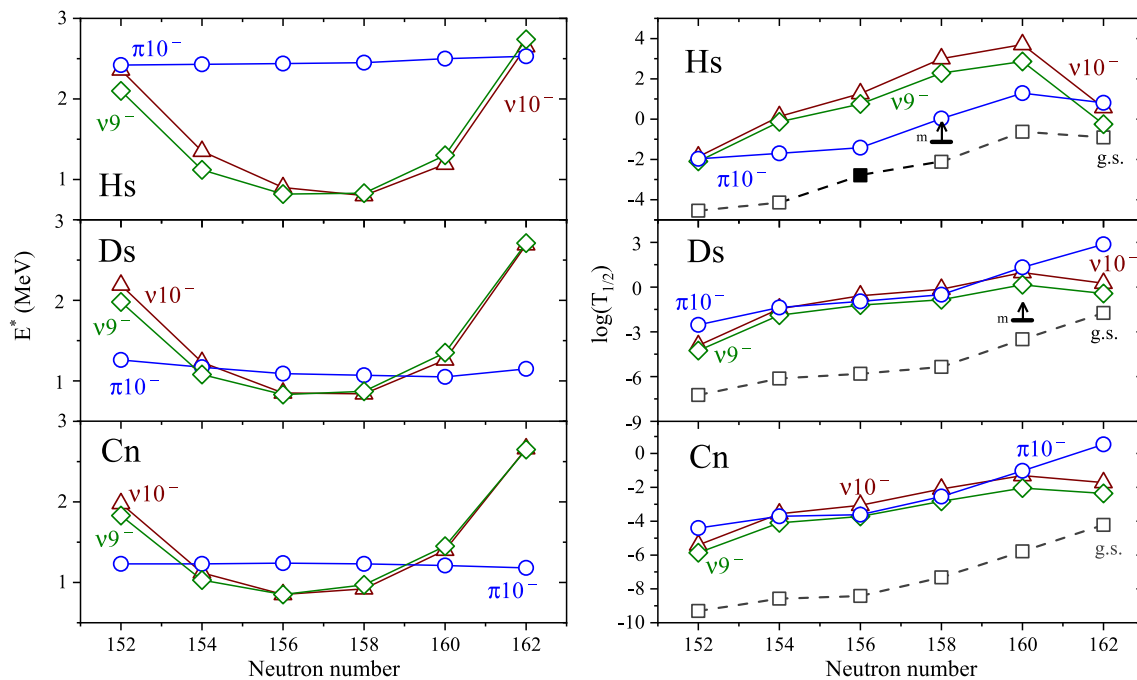
Fig. 8 Excitation energies of theoretically predicted $\nu9^-(7/2^+[613]\otimes 11/2^-[725])$, $\nu10^-(9/2^+[615]\otimes11/2^-[725])$ and $\pi10^-(9/2^-[505]\otimes 11/2^+[615])$ configurations in even–even isotopes of Hs-Cn [50] (left panels). Presently calculated fission half-lives corresponding to these qp-states are shown in the right panels. SF half-lives calculated by using Eqs. (2), (3) and (4) are shown by squares. The experimental partial SF half-life is shown by a filled square. Experimentally measured total half-lives of α-decaying K-isomeric states (noted as m) are shown by horizontal-line symbols and arrows, which indicates that these are considered as lower limits for fission half-lives of high-K states. See text for details

presently predicted to be the most stable configuration among all other intrinsic states including the ground state. The K states are not on the "ground" but rather they are in the "sky", likewise clouds. Thus, they could preferably be called as a "cloud of stability" against fission. Nevertheless, irregardless of terminology, the high-K states in deformed SHN may exist in their own class of many body quantum systems.

The existence of very stable and long-lived high-K states in SHN will shed light on the nuclear stability-landscape in the region of heavy nuclei. Regarding to the possible occurrence of SHN in nature, the high-K states in the odd-A and odd–odd nuclei, which are suggestively be more stable against fission than those in the even–even nuclei are of especial interest. However, high-K states being very stable against fission may still be short-lived as they can decay by other radioactive decay modes. Since these are excited states, they will still decay by electromagnetic and/or α decays. Hence, the total half-life of a K-isomeric state in SHN will be defined by competitions between electromagnetic, α and fission decays.

7 Decay modes and a total half-life of high-K state

Let us briefly estimate the partial half-lives of three different radioactive decay modes in ^{254}Rf and ^{270}Ds, which are representatives of electromagnetic and α decaying K-isomers

from the above two regions of nuclei, i.e., of Fm-Rf and Hs-Ds. In Fig. 9, three different decay scenarios (γ-ray transition, α decay and fission) for the isomeric states in ^{254}Rf and ^{270}Ds are shown schematically. Experimental data on these two isomeric states are scarce, thus, their qp-configurations are assumed to result in 8^- and 9^- states according to predictions from Ref. [50]. In order to make a comparative analysis of their decay modes, the same excitation energy and paths for electromagnetic and α decays were assumed. By attributing 1 MeV excitation energy for both isomers, fission half-lives of about 1×10^{-1} s and 1×10^0 s are calculated for the 8^- and 9^- states, respectively. In the case of a γ-transition, let us assume that in both cases a high-spin (8^+) member of the ground-state rotational band ($K = 0$) at an excitation energy of 0.5 MeV is populated. In both cases, γ quanta with the same energy of 0.5 MeV and multipolarity of E1 should be emitted. However, γ-transitions in ^{254}Rf and ^{270}Ds will be retarded by $\Delta K = 8$ and 9, respectively. By using the most recent parameterizations of $\log(F_K)$ as a function of ΔK given in Ref. [30], half-lives of 7×10^{-3} s and 8×10^{-2} s are calculated for the E1-transitions in ^{254}Rf and ^{270}Ds, respectively. In both nuclei, the half-life of γ-transition is much shorter than the one for fission. Thus, it is unlikely that fission can compete with the electromagnetic decays in both isomeric cases.
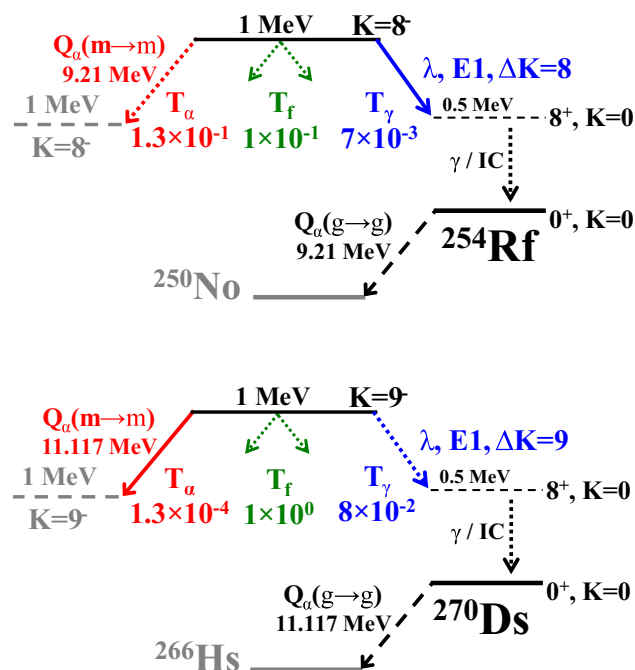
Fig. 9 Schematic illustrations of various de-excitation modes of high-K states in ^{254}Rf and ^{270}Ds. Calculated partial half-lives (in unit of s) for various decay modes are given. Decay schemes for electromagnetic and α transitions from high-K states and their related values are the assumptions, which are used in this work. Only Q_α for the ground to ground state is taken from Ref. [83]. Dashed lines and arrows indicate unknown states and unknown decay branches, respectively. For details see text

Now, for the α decay, let us assume that the same 2-qp state exist in the daughter nuclei at the same excitation energy of 1 MeV. Such an assumption will allow us to use the Q_α value between ground states for the favored α-decay transition [42]. It is worth noting that various theoretical estimates on partial α decays of high-K states including non-favored transitions (e.g., $\Delta K > 0$) exist [49,51,80]. However, we are considering only favored, i.e., the most probable transition, which is sufficient for the present discussion. Half-lives of these α-decays can be calculated by using a semi-empirical approach given in Ref. [81], with improved parameters from Ref. [82]. The ground-to-ground state Q_α values are taken from Ref. [83]. Calculated α-decay half-lives are 1.3×10^{-1} s and 1.3×10^{-4} s for ^{254}Rf and ^{270}Ds, respectively.

In ^{254}Rf, it is evident that α decay cannot compete with γ-ray emission, thus, its main decay mode will be an electromagnetic transition with a total half-life value of up to several ms. Indeed, the experimentally observed K-isomeric state [47,74] decays via an electromagnetic transition with a total half-life of 4 μs, which is shorter than the 20 μs of its fissioning ground state which confirms the above estimate.

In the case of ^{270}Ds, the α-decay half-life is shorter than the half-life of the γ-transition, thus, the most probable de-excitation mode of this 9^- state will be the α decay. One

should mention that this is only possible if a similarly high-K state exists in the daughter ^{266}Hs nucleus. These conclusions are in agreement with experimental data. The α-decaying K isomeric state in ^{270}Ds has been measured [42] and evidence for the presence of a K-isomeric state in ^{266}Hs also exists [48]. Moreover, the experimental α-decay half-life of the K-isomeric state in ^{270}Ds is ≈ 6 ms [42], which is longer than the ≈ 0.1 ms [42] of its α-decaying ground state. Therefore, the experimental data on K-isomeric states in ^{266}Hs and ^{270}Ds, together with the results from the present semi-empirical estimates give hope on the possible existence of more longer lived K-isomeric states in SHN.

Finally, by summarizing all above results and discussions one can conclude that within the presently suggested semi-empirical approach various high-K state phenomena in the heaviest nuclei can well be explained. The present estimates may be a useful tool to guide experimental studies of heavy nuclei.

8 Access to extremely short-lived nuclei via a K-trapping

Present experimental techniques are limited to the direct production of nuclei with half-lives of less than about 1 μs, which is mainly required for their separation at in-flight separators and delivery to a detection system for registration of their radioactive decays [19,84]. Thus, the heaviest nuclei having extremely unstable ground states, e.g., decaying by SF with half-lives shorter than about 1 μs are experimentally inaccessible via direct production. According to the present results, if high-K states would exist in such heavy nuclei then they may have total half-lives of longer than about 1 μs. In this case, the extremely short-lived heavy nuclei can be safely separated and transported to the detection system. Once such a nucleus is delivered to the detection system in its K-isomeric state, the subsequent radioactive decays can be studied together with its ground state as done for the cases of the all known K-isomers [29]. This provides a unique opportunity to study extremely unstable exotic nuclear systems, such as neutron-deficient nuclei, and would help to expand the isotopic map of the nuclei. From the results shown in Fig. 7, such situations may occur and be studied in hitherto unknown and sub-μs ^{248}No, ^{250}Rf and ^{252}Rf isotopes.

With regard to the relevance for the study of extremely short-lived nuclei, it is worth mentioning a recently raised debate on the expected SF half-life for ^{252}Rf. In the analysis of the experimental SF half-lives of Rf isotopes known at that time (prior to Ref. [69]) with a focus on the single-particle shell effect on fission, it was noticed that the SF half-lives of unknown neutron-deficient Rf isotopes with $N < 150$ may soon reach an isotopic boarder, i.e, a value of 10^{-14} s. This was based on the expected SF half-life of less than 1 ps

$(10^{-12}$ s) for ^{252}Rf, which was calculated with the known SF half-lives of neighboring ^{253}Rf and ^{254}Rf isotopes and with a factor of 10^4 for the single-particle effect on the SF half-life of ^{253}Rf. However, new experimental findings in Ref. [69], and its interpretation led to the conclusion that the SF half-life of ^{252}Rf is not on the order of 10^{-12} s but rather $\approx 10^{-7}$ s. Meanwhile, in the recent work [73], where the experimental findings from Ref. [69] have been confirmed but differently interpreted (see discussions made in the previous section), was in favor of the extremely short half-life scenario for ^{252}Rf, which was initially suggested and believed to be disproved in Ref. [69]. In other words, according to Ref. [73], the SF half-life of ^{252}Rf is still suggested to be shorter than 1 ps and, thus, experimentally inaccessible.

The present prediction on ^{252}Rf suggest that experimental access to this nucleus can be found via its a high-K state (e.g., $K = 6$, see Fig. 7). In the present work, a SF half-life of about 1 μs was calculated. As already mentioned in the previous section, this value could be overestimated because for its calculation the curvature energy of ^{254}Rf was used (see discussions in the previous section). In fact, a similarly high value of 0.63 μs has been predicted in a pure theoretical calculation [85].

Nevertheless, to examine the possible transport/access of this nucleus, let us consider two different empirically estimated SF half-life values of about 0.1 μs and 1 ps for ^{252}Rf, which were given in Ref. [69]. By describing these values within the present semi-empirical approach (see previous section), $(\hbar\omega)_{SF} = 1.95$ and 6.6 MeV are extracted in cases of 0.1 μs and 1 ps, respectively. This leads to two extremely different scenarios for the shape of a 5.09 MeV-high fission barrier in ^{252}Rf [59]. It should be mentioned that $(\hbar\omega)_{SF} = 6.6$ MeV is an unprecedentedly large value (cf. Fig. 2), which is unlikely to be a realistic.

Nevertheless, one can calculate the fission half-lives of the above-mentioned $K = 6$ state in ^{252}Rf by taken these two $(\hbar\omega)_{SF}$ values. The values of 50 μs and 3 ns are estimated by using the $(\hbar\omega)_{SF} = 1.95$ and 6.6 MeV, respectively. This shows that the high-K state in ^{252}Rf will provide experimental access to this nucleus only in the case if its ground state SF half-life is about 0.1 μs or longer. If so, then with the current availability of fast digital electronics [45,47,74], the ground-state fission of ^{252}Rf can be disentangled from the de-excitation of K-isomeric state down to a time scale of about 0.1 μs [84]. In summary, if the conclusion made in Ref. [69] is a correct, then the unknown ^{252}Rf may still have a chance to be discovered, not only at its high-K state, but also at its ground state.

9 Summary and conclusion

In the present work, fission from high-K states formed in couplings of quasiparticles in SHN was discussed and described within the semi-empirical approach. A semi-empirical expression for the estimation of fission-hindrance factor relative to unhindered fission half-lives of high-K states was suggested. The fission half-lives were calculated for various theoretically predicted high-K states in Fm-Rf and Hs-Ds. It has been found that high-K states in SHN seem to be more stable against fission compared to their ground state. Discussion of the obtained results led to predictions of different interesting and intriguing physics scenarios, which could occur in SHN. Some predictions were found to be in good agreement with the experimental observations, such as α-decay of the K isomeric state in ^{270}Ds, and long half-life of K isomer in ^{250}No etc. The existence of high-K states in SHN would help to expand the experimentally known nuclear chart towards extremely unstable cases, such as very neutron-deficient SHN. Moreover, the existence of high-K states in neutron-rich SHN, which could be produced in the nuclear astrophysical process are of great interest within the framework of the possible occurrence of superheavy elements in nature. For this, one needs to have theoretical predictions for possible multi-qp configurations with high-K numbers in odd-A, odd–odd, and neutron-rich SHN that are relevant to the astrophysical r-process.

Data Availability Statement All necessary and discussed data are provided in the paper.

References

1. R. Vandenbosch, J.R. Huizenga, *Nuclear Fission* (Academic Press, New York and London, 1973)
2. A.N. Andreyev, K. Nishio, K.H. Schmidt, Rep. Prog. Phys. **81**(1), 016301 (2017)
3. M. Bender, R. Bernard, G. Bertsch, S. Chiba, J. Dobaczewski, N. Dubray, S.A. Giuliani, K. Hagino, D. Lacroix, Z. Li, P. Magierski, J. Maruhn, W. Nazarewicz, J. Pei, S. Péru, N. Pillet, J. Randrup, D. Regnier, P.G. Reinhard, L.M. Robledo, W. Ryssens, J. Sadhukhan, G. Scamps, N. Schunck, C. Simenel, J. Skalski, I. Stetcu, P. Stevenson, S. Umar, M. Verriere, D. Vretenar, M. Warda, S. Åberg, J. Phys. G Nucl. Part. Phys. **47**(11), 113002 (2020)
4. E. Fermi, Nature **133**, 898 (1934)
5. O. Hahn, F. Strassmann, Naturwissenschaften **27**, 11 (1939)
6. L. Meitner, O. Frisch, Nature **143**, 471 (1939)
7. N. Bohr, J.A. Wheeler, Phys. Rev. **56**, 426 (1939)
8. G. Flerov, K. Petrzhak, Phys. Rev. **89**, 58 (1940)
9. D.L. Hill, J.A. Wheeler, Phys. Rev. **89**, 1102 (1953)
10. A. Wapstra, Pure Appl. Chem. **63**, 879 (1991)
11. V. Strutinsky, Nucl. Phys. A **95**, 420 (1967)
12. S. Bjornholm, J. Lynn, Rev. Mod. Phys. **52**, 725 (1980)
13. F.G. Werner, J.A. Wheeler, Phys. Rev. **109**, 126 (1958)
14. S. Hofmann, S.N. Dmitriev, C. Fahlander, J.M. Gates, J.B. Roberto, H. Sakai, Pure Appl. Chem. **92**, 1387 (2020)
15. A. Sobiczewski et al., Phys. Lett. **22**, 500 (1966)
16. W. Myers, W. Swiatecki, Nucl. Phys. **81**, 1 (1966)
17. S.G. Nilsson, C.F. Tsang, A. Sobiczewski, Z. Szymański, S. Wycech, C. Gustafson, I.L. Lamm, P. Möller, B. Nilsson, Nucl. Phys. A **131**, 1 (1969)
18. A. Sobiczewski, K. Pomorski, Prog. Part. Nucl. Phys. **58**, 292 (2007)
19. S. Hofmann, G. Münzenberg, Rev. Mod. Phys. **72**(3), 733 (2000)
20. Yu Ts. Oganessian, A. Sobiczewski, G.M. Ter-Akopian, Phys. Scr. **92**(2), 023003 (2017)
21. J. Khuyagbaatar et al., EPJ Web Conf. **131**, 03003 (2016)
22. F.P. Hessberger, Eur. Phys. J. A **53**, 75 (2017)
23. J. Randrup, C. Tsang, P. Möller, S. Nilsson, S. Larsson, Nucl. Phys. A **217**, 221 (1973)
24. Z. Lojewski, A. Baran, Z. Phys. A **322**, 695 (1985)
25. P. Jachimowicz, M. Kowal, J. Skalski, Phys. Rev. C **92**, 044306 (2015)
26. P. Walker, F.R. Xu, Phys. Scr. **91**, 1 (2016)
27. S.G. Nilsson, Dan. Mat.-Fys. Medd. **29**(16), 1–69 (1955)
28. F. Xu, E. Zhao, R. Wyss, P. Walker, Phys. Rev. Lett. **92**, 252501 (2004)
29. D. Ackermann, C. Theisen, Phys. Scr. **92**, 083002 (2017)
30. F. Kondev, G. Dracoulis, T. Kibédi, At. Data Nucl. Data Tab. **103–104**, 50 (2015)
31. P. Walker, G. Dracoulis, Nature **399**, 35 (1999)
32. J. Khuyagbaatar, EPJ Web Conf. **163**, 00030 (2017)
33. A. Lopez-Martens, K. Hauschild, and the GABRIELA collaboration, Eur. Phys. J. A **58**(7), 134 (2022)
34. R.D. Herzberg, P. Greenlees, Prog. Part. Nucl. Phys. **61**(2), 674 (2008)
35. A. Baran, Z. Łojewski, Phys. Lett. B **176**, 7 (1986)
36. A. Baran, Z. Łojewski, Nucl. Phys. A **475**, 327 (1987)
37. Y.A. Lazarev, Y.V. Lobanov, R.N. Sagaidak, V.K. Utyonkov, M. Hussonnois, Y.P. Kharitonov, I.V. Shirokovsky, S.P. Tretyakova, Y.T. Oganessian, Phys. Scr. **39**(4), 422 (1989)
38. P.M. Walker, F.R. Xu, H.L. Liu, Y. Sun, Nucl. Part. Phys. **39**(10), 105106 (2012)
39. H.L. Liu, F.R. Xu, P.M. Walker, C.A. Bertulani, Phys. Rev. C **83**, 011303 (2011)
40. H.L. Hall et al., Phys. Rev. C **39**, 1866 (1989)
41. F.P. Hessberger et al., Eur. Phys. J. A **43**, 55 (2009)
42. S. Hofmann, F.P. Hessberger et al., Eur. Phys. J. A **10**, 5 (2001)
43. D. Peterson, B.B. Back, R.V.F. Janssens, T.L. Khoo, C.J. Lister, D. Seweryniak, I. Ahmad, M.P. Carpenter, C.N. Davids, A.A. Hecht, C.L. Jiang, T. Lauritsen, X. Wang, S. Zhu, F.G. Kondev, A. Heinz, J. Qian, R. Winkler, P. Chowdhury, S.K. Tandel, U.S. Tandel, Phys. Rev. C **74**, 014316 (2006)
44. A. Svirikhin et al., Phys. Part. Nucl. Lett. **14**, 571 (2017)
45. J. Kallunkathariyil et al., Phys. Rev. C **101**, 011301 (2020)
46. J. Khuyagbaatar et al., Phys. Rev. C **106**, 024309 (2022)
47. H.M. David et al., Phys. Rev. Lett. **115**, 132502 (2015)
48. D. Ackermann et al., GSI Sci. Rep. **2011**, 208 (2012)
49. G.G. Adamian, N.V. Antonenko, W. Scheid, Phys. Rev. C **81**, 024320 (2010)
50. H.L. Liu, P.M. Walker, F.R. Xu, Phys. Rev. C **89**, 044304 (2014)
51. P. Jachimowicz, M. Kowal, J. Skalski, Phys. Rev. C **98**, 014320 (2018)
52. J. Khuyagbaatar, Eur. Phys. J. A **55**, 134 (2019)
53. J. Khuyagbaatar, Nucl. Phys. A **1002**, 121958 (2020)
54. V.F. Weisskopf, Phys. Rev. **83**, 1073 (1951)
55. L. Rusinov, Usp. Fis. Nauk **73**, 615 (1961)
56. K. Löbner, Phys. Lett. B **26**, 369 (1968)
57. A. Baran, M. Kowal, P.G. Reinhard, L. Robledo, A. Staszczak, M. Warda, Nucl. Phys. A **944**, 442 (2015)
58. V. Viola, B. Wilkins, Nucl. Phys. **82**, 65 (1966)
59. P. Möller et al., Phys. Rev. C **91**, 024310 (2015)
60. V. Zagrebaev, W. Greiner, Nucl. Phys. A **944**, 257 (2015)
61. S. Goriely, S. Hilaire, A.J. Koning, M. Sin, R. Capote, Phys. Rev. C **79**, 024612 (2009)
62. Y. Oganessian et al., Nucl. Phys. A **239**, 157 (1975)
63. M. Warda, J.L. Egido, Phys. Rev. C **86**, 014322 (2012)
64. P. Möller et al., Phys. Rev. C **79**, 064304 (2009)
65. G.T. Seaborg, Phys. Rev. **85**, 157 (1952)
66. P. Möller et al., At. Data Nucl. Data Tab. **59**, 185 (1995)
67. http://www.nndc.bnl.gov/ensdf/
68. D.A. Shaughnessy et al., Phys. Rev. C **63**, 037603 (2001)
69. J. Khuyagbaatar et al., Phys. Rev. C **104**, L031303 (2021)
70. F.P. Hessberger et al., Eur. Phys. J. A **58**, 11 (2022)
71. J.P. Delaroche, M. Girod, H. Goutte, J. Libert, Nucl. Phys. A **771**, 103 (2006)
72. K. Kessaci, B.J.P. Gall, O. Dorvaux, A. Lopez-Martens, R. Chakma, K. Hauschild, M.L. Chelnokov, V.I. Chepigin, M. Forge, A.V. Isaev, I.N. Izosimov, D.E. Katrasev, A.A. Kuznetsova, O.N. Malyshev, R. Mukhin, J. Piot, A.G. Popeko, Y.A. Popov, E.A. Sokol, A.I. Svirikhin, M.S. Tezekbayev, A.V. Yeremin, Phys. Rev. C **104**, 044609 (2021)
73. A. Lopez-Martens et al., Phys. Rev. C **105**, L021306 (2022)
74. J. Khuyagbaatar et al., Nucl. Phys. A **994**, 121662 (2020)
75. P. Mosat et al., Phys. Rev. C **101**, 034310 (2020)
76. H.B. Jeppesen et al., Phys. Rev. C **79**, 031303 (2009)
77. J. Khuyagbaatar et al., Phys. Rev. C **103**, 064303 (2021)

78. N. Minkov, L. Bonneau, P. Quentin, J. Bartel, H. Molique, D. Ivanova, Phys. Rev. C **105**, 044329 (2022)
79. M. Tezekbayeva et al., Eurasian J. Phys. Funct. Mater. **3**, 300 (2019)
80. R.M. Clark, D. Rudolph, Phys. Rev. C **97**, 024333 (2018)
81. D. Poenaru, Ivaşcu, D. Mazilu, J. Phys. Lett. **41**, L (1980)
82. E. Rurarz, Act. Phys. Pol. **14**, 917 (1983)
83. M. Wang et al., Chin. Phys. C **41**, 030003 (2017)
84. J. Khuyagbaatar et al., Phys. Rev. Lett. **115**, 242502 (2015)
85. R. Smolanczuk, J. Skalski, A. Sobiczewski, Phys. Rev. C **52**, 1871 (1995)